Analysis of Uncertainty in p_T and its Effects on Dimuon Invariant Mass Yield in the CMS Detector

Tamra M. Nebabu
Duke University
SIST Intern

Dr. Pushpalatha Bhat, Dr. Leonard Spiegel
Fermi National Accelerator Laboratory

Abstract

In the search for physics beyond the standard model, it is especially important to be mindful of the uncertainty associated with various measurements when interpreting the results of a collision experiment. This study examines a potential systematic error in the CMS detector. In particular, this study investigated the possibility of a momentum-dependent bias in the curvature measurements of the detector caused by a geometrical weak mode. This bias can cause uncertainty in transverse momentum (p_T) measurements for muons, which can propagate into uncertainty in the reconstructed dimuon mass spectrum. By using the cosmic muon data collected in 2015, the study was able to demonstrate that the curvature bias in the CMS detector is minimal, causing an apparent curvature shift of 0.01 ± 0.07 C/TeV. This bias translates into a scaling factor for p_T that increases as 0.001% of the p_T in GeV. However, the uncertainty that results from this bias disproportionately affects high-p_T muons, and as a result, propagates into larger uncertainties in the observed yield of high-mass dimuons. Because evidence for compositeness would appear in the high-mass regions of the spectrum, it is essential to quantify the uncertainty in this yield. Using $q\bar{q} \rightarrow \mu^+\mu^-$ collision events generated in Pythia8, the effects of a p_T uncertainty in the dimuon mass spectrum were quantified.

1 Introduction

1.1 CMS Detector

A hundred meters underground in the small agricultural commune of Cessy, France resides a massive cylindrical onion of metal detectors known as the Compact Muon Solenoid (CMS) (see Figure 1). It is one of two general purpose detectors at the Large Hadron Collider (LHC), which is currently the world's largest particle collider. Spanning a diameter of 15 meters and a length of 21 meters, the CMS detector is the second largest particle detector by volume[1]. However, it is the heaviest detector in the world, weighing about fourteen thousand metric tonnes. The primary role of CMS is to detect the showers of particles that result from high-energy hadron-hadron collisions. By identifying and tracking these outgoing particles, physicists can make inferences about the nature of the interactions that give rise to the outgoing particles.

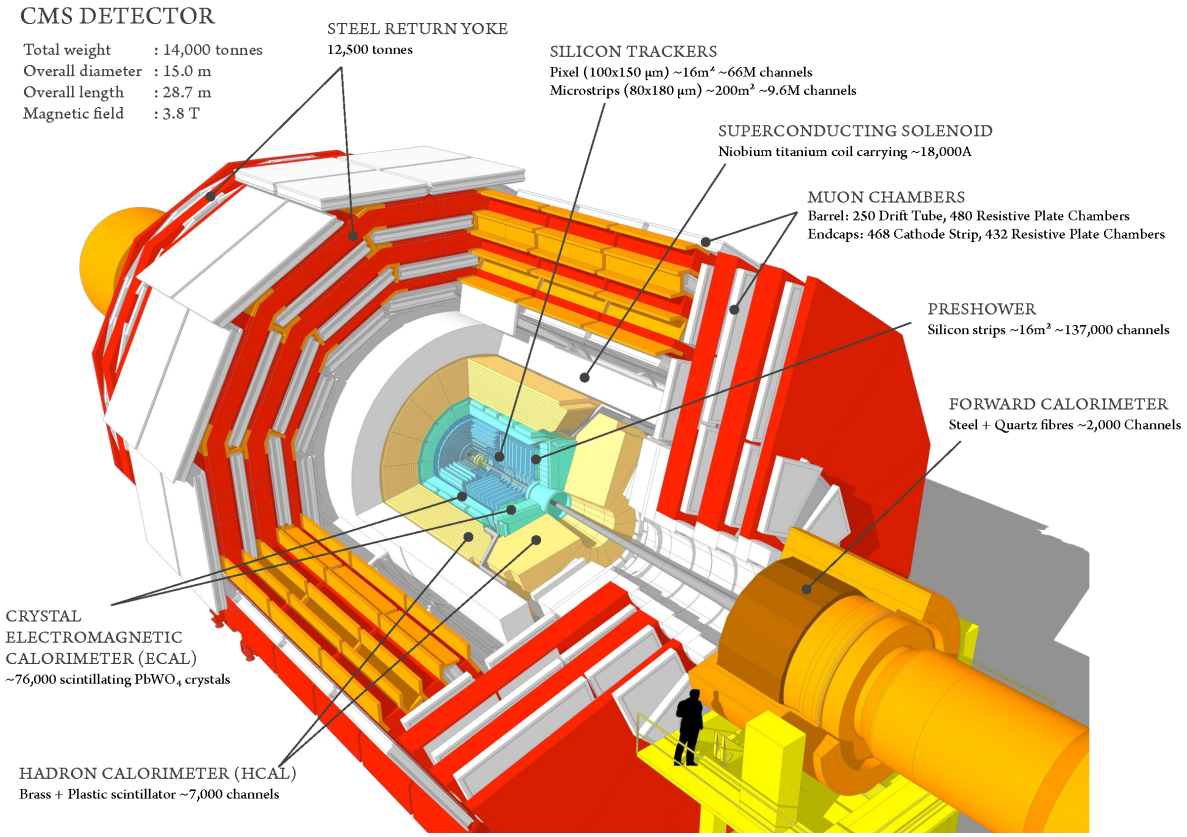

Figure 1: General Schematic of the CMS Detector[1]

The CMS detector consists of five main layers of specialized detection modules, which extend radially outward from the cylindrical beamline (see Figure 2). In order from the innermost part of the detector to the outermost part, these modules are as follows:

1. Silicon tracker
2. Electromagnetic Calorimeter (ECAL)
3. Hadron Calorimeter (HCAL)
4. Superconducting Magnet
5. Muon Detectors and Return Yoke[2]

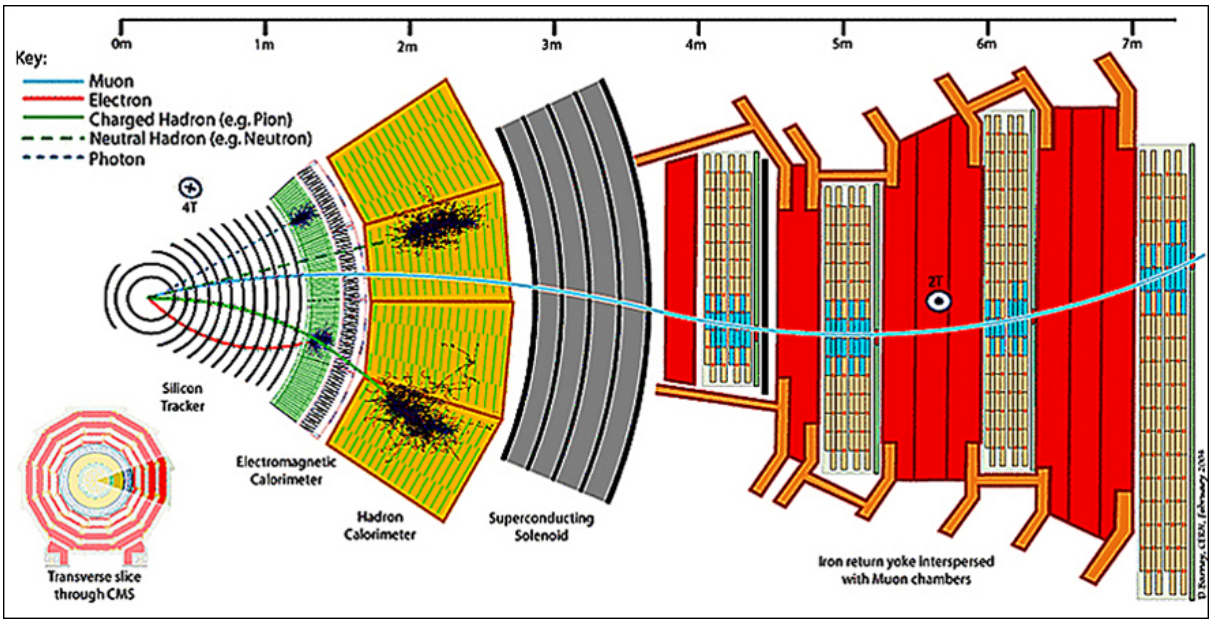

Figure 2: Cross-Sectional Layers of the CMS Detector and Particle Tracks[2]

The silicon tracker is composed of three inner layers of silicon "pixels" and ten outer layers of silicon strips. Each pixel has dimensions of about 100 microns by 150 microns and each module of the strip, giving the inner part of the silicon detector a remarkably high granularity[3]. When a charged particle passes through the tracker, its electric field imparts enough energy to liberate electrons from the silicon atoms, and these freed electrons are redirected to generate a current readout. Thus, the silicon tracker is able to locate which pixels the charged particles passed through and reconstruct their paths from the collision point in the beamline.

All of the remaining chambers in the detector are designed to directly or indirectly measure the energy of the particles produced in the collision. The electromagnetic calorimeter (ECAL) is composed of thousands of lead tungstate crystals and photodetectors that track and measure the energy of outgoing electrons and photons[4]. The crystal is a scintillator material, which means it luminesces when its electrons are excited by incoming high-energy particles. This light can then be collected by the photodetectors and converted into an electronic signal for readout. Electrons and photons leave "light tracks" in ECAL, and are eventually halted as they lose energy to the densely-packed crystalline atoms. In contrast, hadrons and muons leave little to no energy in ECAL because they generally possess so much energy that they pierce through the calorimeter without exciting the crystalline atoms. As such, the ECAL behaves like a light-based version of the silicon tracker for these particles. Furthermore, because the amount of light emitted by the scintillator is proportional to the energy of the incoming particle, the calorimeter also operates as an energy-measuring device.

Next, the hadron calorimeter (HCAL) is used to measure the energy of outgoing hadrons. The hadrons that pass through ECAL are slowed and stopped by dense layers of scintillator and absorber materials in HCAL. The absorbing material—generally brass or steel—causes the hadrons to decay into a"shower" of secondary particles, which then cause the scintillator to emit light[5]. As in the ECAL, this light is captured by photodetectors and processed to figure out the energy.

All of the particle identification and path reconstruction in the detector is enabled by the presence of the superconducting solenoidal magnet, which is the namesake of CMS. It generates

a magnetic field of 4 Tesla parallel to the beamline axis, and this field flows in opposite directions on the inside and outside of the solenoid. This allows particles to be identified based on how they move through the magnetic field. Any charged particle moving through the field experiences a force perpendicular to its motion, causing the particle to travel in a curved path. The direction of curvature is related to the sign of the particle's charge whereas the amount of curvature is inversely related to the particle's momentum. For example, protons will curve in the opposite direction to electrons, and high-energy muons will be deflected less than low-energy hadrons.

The final outermost layer of the detector consists of a series of tiled gas chambers which track the muons that pass through. These high-energy muons are deflected by the magnetic field of the solenoid, which is greatly enhanced by the presence of the iron in the steel. As they travel in curved paths through the chambers, they ionize gas molecules along the way. The ionized electrons are then collected by a positively charged wire running through each of the gas chambers, and are converted into an electrical signal that pinpoints the 2D location of the muon. The properties of the muons such as their energy and charge are inferred by analyzing their curvature through the muon detector.

1.2 Cosmic Muons versus Collision Muons

Although the CMS detector is primarily designed for collision analysis, it can also be configured to collect data from cosmic particles that are created in the upper atmosphere. This is especially advantageous because of the wealth of cosmic data and its overall predictability, which make it suitable for detector performance studies. Because the CMS collaboration is particularly interested in muons, many of the cosmic studies that are conducted involve cosmic muons. These cosmic muons are generally very high in energy and pass in and out of the detector, leaving tracks in the very same chambers as their collision-born counterparts. However, because these cosmics originate above the detector rather than in the beamline, they follow a very different trajectory than the collision muons. In fact, depending on the angle at which the cosmic muons enter the top of the detector, they may only pass through the outer muon detection layer, or be deflected significantly as they pass through the middle of the solenoid (see Figure 3). In the latter case, the differential magnetic field on either side of the solenoid causes the muon to appear to have two separate tracks, which are often labeled the upper leg and lower leg.

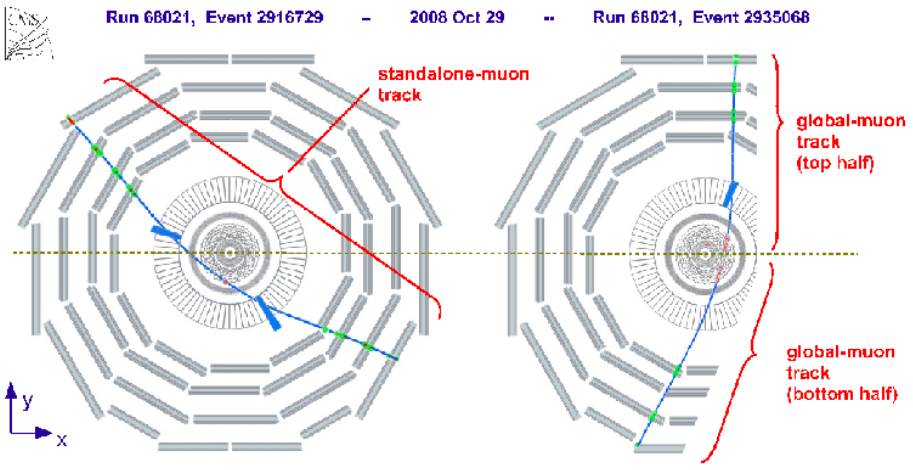

Figure 3: Possible Trajectories of Cosmic Muons in the Detector[3]

1.3 Objectives

One of the primary goals of CMS is to search for evidence of exotic particles and physics beyond the standard model. However, as with any search for never-observed phenomena, one must be cautious when evaluating the uncertainty of the measurements and making an unbiased interpretation of the results. For this reason, much emphasis is placed on simulations, so that physicists may be able to get an idea of what kind of results to expect. Furthermore, this allows experimentalists to design the experiment's specifications to cover the bandwidth of possible results. This focuses the experiment, and makes it easier to make conclusive statements about the data that is collected. In the spirit of this approach, the studies detailed in this paper use simulation to evaluate the uncertainty in experimentally collected data. The first part of the study compared experimental cosmic muon data to monte carlo simulations to search for bias in the detector's measurements, and the second part of the study used simulations to predict how this bias would propagate into uncertainty in mass distributions of collision particles.

1.4 Tools of the Trade

The monte carlo simulations used in the first part of the study were taken from the CMS Monte Carlo Reference Database. These simulations were then analyzed along with cosmic muon data collected in 2015 with ROOT 6.06/02. For the second part of the study, collision events were generated in Pythia8 and analyzed with the same ROOT release.

2 Uncertainty in the Tranverse Momentum p_T

2.1 Cosmic Endpoint Method

The Cosmic Endpoint Method is an analysis technique for evaluating the potential curvature bias in the detector[7]. It presumes that this bias manifests as a constant shift in curvature, which can be resolved into a p_T-dependent scaling of p_T (see Appendix A). The motivation for this presumption lies in the possibility of a geometric distortion in the detector, which would generate a weak mode that affects the detector's measurements in a predictable way[6]. To see if this is indeed the case, the method uses monte carlo simulations of cosmic muons to check whether or not the detector is in need of calibration. First, a bias is injected into the simulation data by adding (or subtracting) a constant to all of the curvature values. Then the χ^2 between the experimental data and the shifted simulation data is calculated to see how much they differ. This process is repeated for a range of shifts, and the shift at which the χ^2 is minimized (i.e. where there is the most agreement between the experiment and simulation) is taken to be the bias in the detector. This bias is effectively the "distortion" that one must apply to a theoretically unbiased set of simulated values in order to generate the measured results.

It should be noted that because the Cosmic Endpoint Method is contingent on the monte carlo simulations producing unbiased results, the size of the simulated data set must be large enough to produce good statistics. However, because the method generally uses histogram distributions of curvature to compare the experimental data to simulation, the two data sets need not be comparable in size to each other, but should be normalized accordingly.

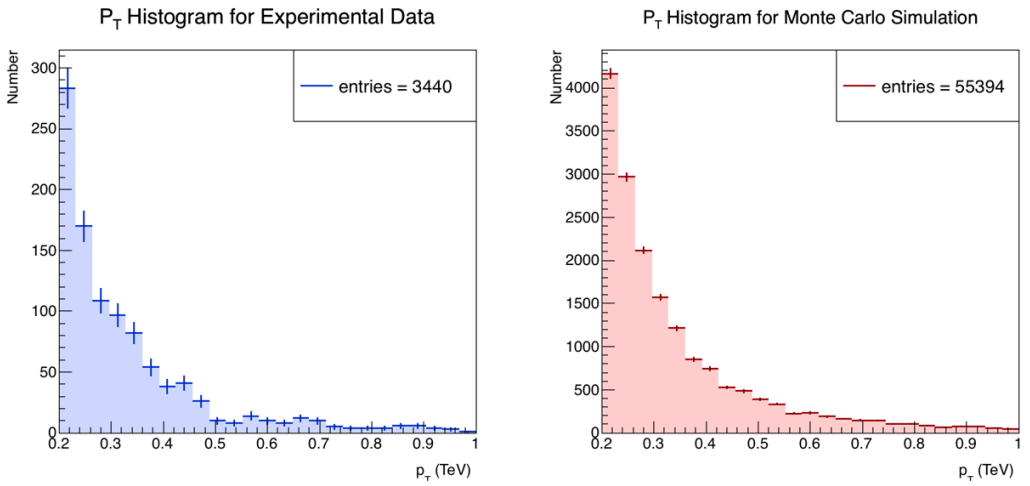

(a) p_T Histograms

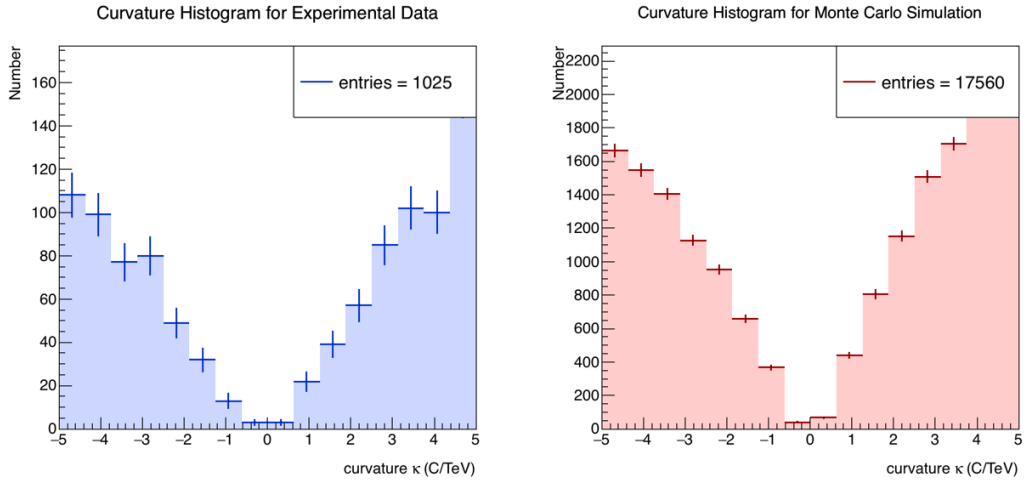

(b) Curvature Histograms

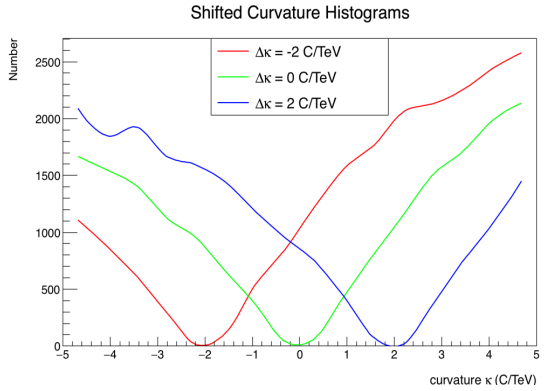

(c) Example Curvature Histograms with Injected Bias

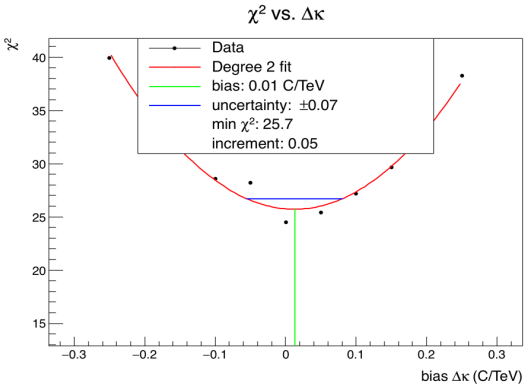

(d) χ^2 vs. Injected Bias

Figure 4: **General Procedure of Cosmic Endpoint Method**: Subfigure 4a shows the raw histograms obtained using the 2015 CRAFT data and Asymptotic monte carlo simulation. The same data was used to produce the curvature histograms shown in 4b. The simulation curvature data was shifted by a spectrum of biases, and a few examples of the resulting histograms are shown as curves in Figure 4c. These shifted histograms were compared to the curvature histograms of the data, and the amount of disagreement between the histograms was quantified in the χ^2 vs. injected bias plot in 4d.

2.2 Procedure

First, p_T histograms were constructed for both the experimental and simulated cosmic muon data using an average of the upper and lower tracks. Because the muon's decay time is exponentially distributed[8], and because cosmic muons radiate away energy as they travel to the surface of the Earth, it is expected that their transverse momentum distributions are also exponentially decaying. This can be seen in the plot in Figure 4a. Next, the p_T values were used to build histograms of the muons' curvature κ, which is defined as the charge of the muon divided by its transverse momentum. Motivation for this definition is presented in Appendix B. Since there is a higher incidence of low-p_T muons than high-p_T muons, there should be more muons with high curvatures than low curvatures. Furthermore, because the charge of a muon can take on values of ± 1, the curvature distribution should be roughly symmetric across the y-axis, as is the case in Figure 4b. A strict magnitude cutoff of 0.005 C/GeV or 5 C/TeV was applied to the curvature histograms to restrict the range of muons analyzed to those with high p_T.

Before comparing the curvature histograms of the experimental data and simulation, they were normalized to have the same proportion of positive and negative muons. Because the parent particle of the cosmic muons is a proton (which is positively charged), there will be more positive muons produced than negative muons. This inherent asymmetry causes the right half of the curvature histograms to contain more entries than the left. As a result, when scaling the simulation data down to contain the same number of entries as the data, one should use *two* different scaling factors for the positive and negative muons. Thus, the scaled simulation histogram will have the same number of positive and negative entries as the experimental data.

Next, a bias was injected into the curvature histogram produced by the simulation data. This was done by shifting each *entry* in the histogram by a constant amount $\Delta\kappa$. The shifted curvature histogram of the simulation was then compared to the curvature histogram of the experimental run by calculating the χ^2 on a bin-by-bin basis. As such, it was imperative to ensure that the curvature histograms spanned the same range and contained the same number of bins. The definition of χ^2 used for this analysis is defined below:

$$\chi^2 = \sum_{\text{bins}} \frac{(\text{observed} - \text{expected})^2}{(\text{observed} + \text{expected})/2} \tag{1}$$

where the observed and expected values represent the heights of the bins in the data and simulation histograms, respectively. It should be noted that this definition is a modified version of the standard statistical definition of χ^2, and the reason for this is twofold. First, dividing the squared residuals by the *average* of the observed and expected values rather than just the expected value offers protection against the case where either value is 0. This is a possibility if the data sets are binned too finely so as to generate zero-entry bins in the high-p_T/low curvature regions, which have fewer entries on the whole. The second reason for using this modified definition of χ^2 is that the presence of both the observed and expected values in the denominator eliminates the need for partiality between the data sets. Consequently, if the data sets were to be interchanged, the χ^2 value would remain the same. However, an argument can be made for using only the expected value in the denominator, as in the case for the traditional definition of χ^2:

$$\chi^2 = \sum_{\text{bins}} \frac{(\text{observed} - \text{expected})^2}{\text{expected}} \tag{2}$$

This definition may be preferable if one considers the effects of bias injection into the simulation. If the Cosmic Endpoint Method aims to compare the χ^2 values of different injected biases, then

these χ^2 values must be normalized to the same expected value. That is to say, the denominator should not change as a function of the injected bias because one is always comparing the shifted simulation values to the same experimental values. Thus, it makes sense to label the experimental values as the "expected" data set and the simulation values as the "observed" data set. However, in the case where the denominator is an average of the observed and expected values, this average may change slightly with the bias, causing the χ^2 vs. bias plot to be less smooth.

Once this plot was produced, a polynomial was fit to the region near the minimum χ^2. The curvature bias in the detector was taken to be the injected bias at which the χ^2 is minimized. The uncertainty in this value was defined as the amount the minimizing bias would have to change to increment the minimum χ^2 by 1. In this analysis, a quadratic polynomial was fit to the graph, so the upper and lower uncertainties were identical.

2.3 Results

The Cosmic Endpoint Method was performed on the 2015 CRAFT run and 2015 Asymptotic monte carlo data. The results for using the definition of χ^2 presented in Eq. 1 are shown in Figure 5.

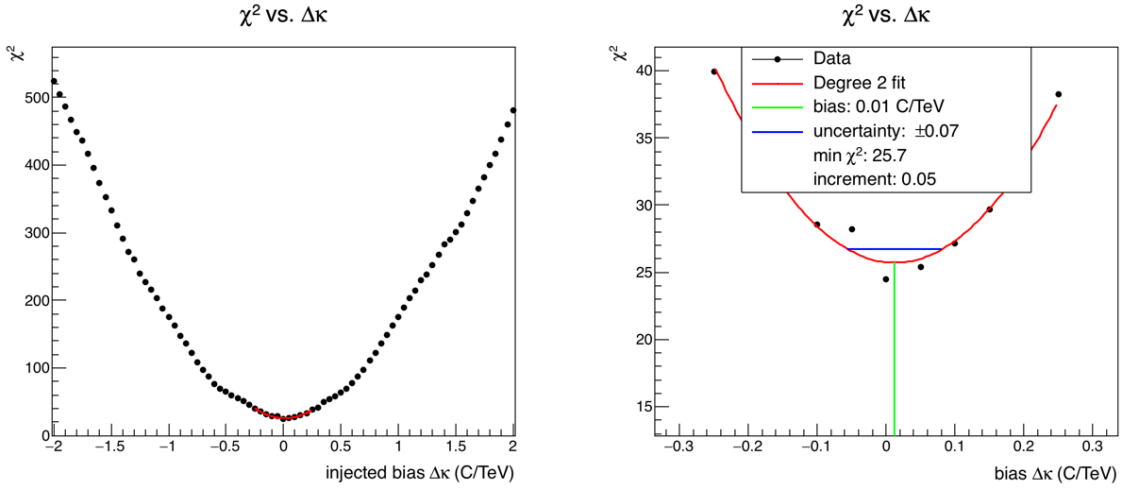

Figure 5: χ^2 **vs. Injected Bias plots**: The plot on the left shows a zoomed-out version of the χ^2 plot, whereas the plot on the right shows a zoomed-in version with the bias, uncertainty, and fit labeled.

As the plots indicates, the apparent curvature bias of the detector is about 0.01 C/TeV with an uncertainty of 0.07 C/TeV. This bias translates into a scaling factor for p_T that increases linearly by 0.001 times the p_T in GeV.

If the definition of χ^2 presented in Eq. 2 is used, the calculated bias becomes 0.002 ± 0.06 C/TeV. Although this bias is an order of magnitude smaller, it is within the range of uncertainty of the first result. Furthermore, the uncertainties in both cases are very close, and ultimately it is this value that will determine the amount of uncertainty in the yield of the dimuon mass spectrum.

2.4 Evaluating the Robustness of the Method

Ideally, the results of the Cosmic Endpoint Method would be more or less independent of the method's parameters. These parameters include but are not limited to the number of bins

in the curvature histograms, the track of muon used, and the increment with which to sweep through various injected biases. To validate the robustness of the method, several tests were devised to check whether the bias and uncertainty varied significantly with each of the parameters.

The first parameter that was examined was the number of bins in the curvature histograms. Because the χ^2 is calculated on a bin-by-bin basis, the number of bins controls how many terms contribute to the χ^2 value. To test the results' dependency on the bin number, the analysis was run on the same data sets for a spectrum of bin numbers while holding all of the other variables constant. The results were obtained using the lower leg of the muon track and are shown in the figure below.

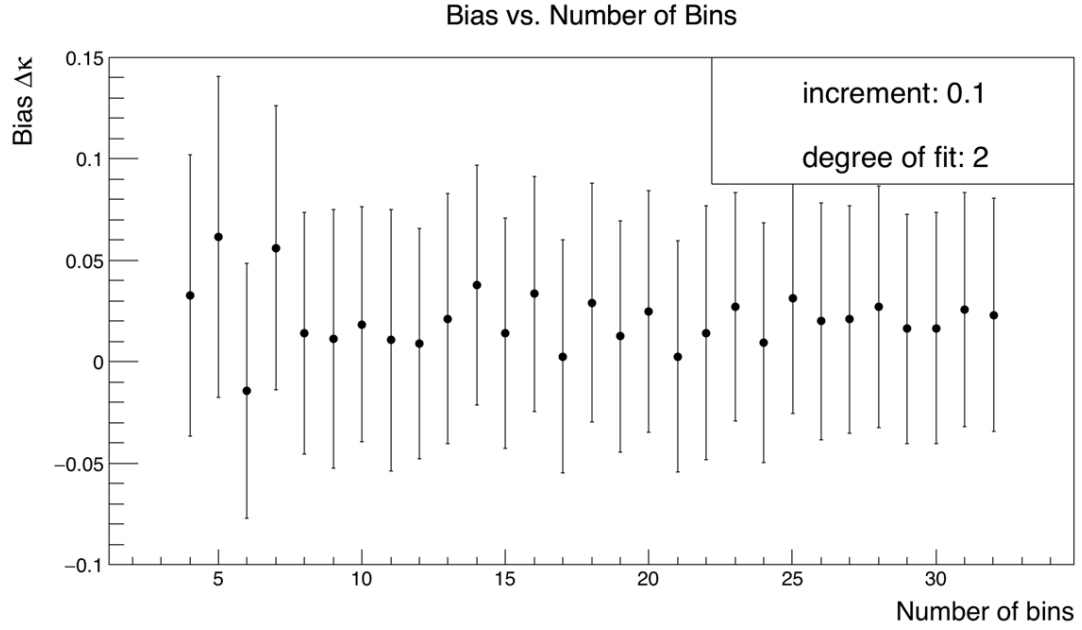

Figure 6: Testing Bin Number Dependence

As the figure demonstrates, there is little variation in the apparent bias of the detector, and the uncertainty is fairly consistent throughout. Thus, for a reasonably large data set, the results of applying the Cosmic Endpoint Method change little with the bin number.

The second parameter that was tested was the increment in the injected biases used to shift the curvature histogram of the simulation. This increment defines the density of points in the χ^2 plot, and consequently, may affect the polynomial fit near the minimum χ^2. The bias and uncertainty are plotted for various increments in Figure 7. As the plot demonstrates, there is almost no variation in the bias and uncertainty up to about 0.4 C/TeV. Above this value however, the bias becomes more unpredictable, and the uncertainty becomes larger. This behavior is to be expected because the higher the increment size, the fewer injected biases are tested and the fewer points there are to fit near the minimum χ^2. Consequently, the fit may not be a good representation of the data, yielding a bias that is far from the actual bias in the detector.

Because cosmic muons deposit little energy in the detector's chambers, there should be a negligible difference in the p_T values for the upper track when they enters the detector and lower track when they leave the detector. Thus, the apparent bias and uncertainty should be the same for both tracks. To confirm this, the Cosmic Endpoint Method was run using the p_T of

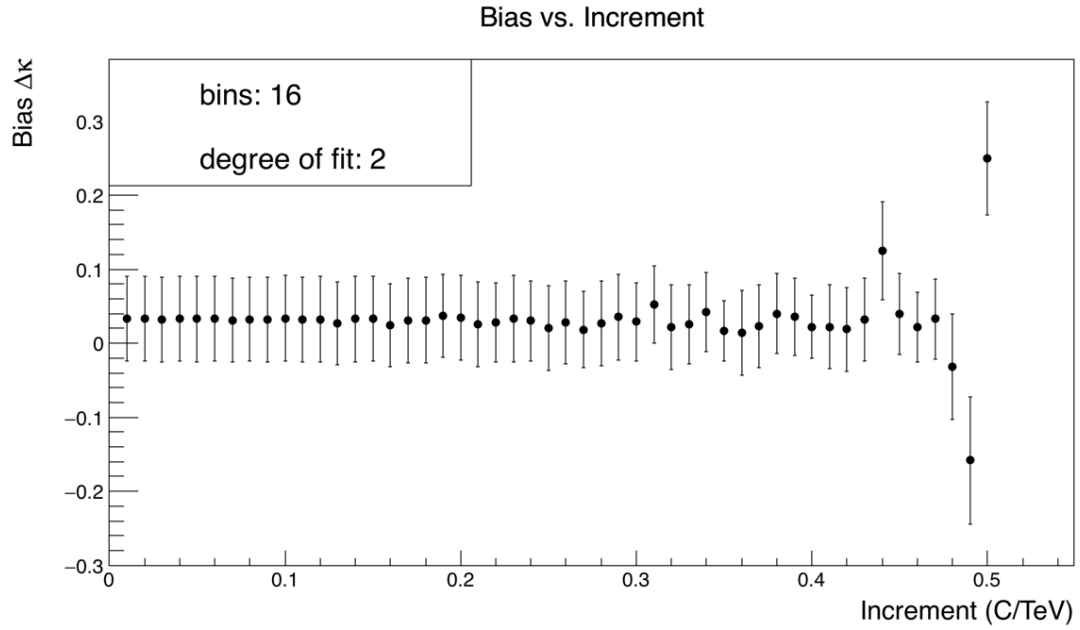

Figure 7: Testing Dependence on the Increment in the Injected Bias

the upper leg, lower leg, and an average of the two. As Figure 8 demonstrates, the calculated uncertainty was the same in all three cases (±0.08 C/TeV) and the biases were all within this uncertainty range of each other.

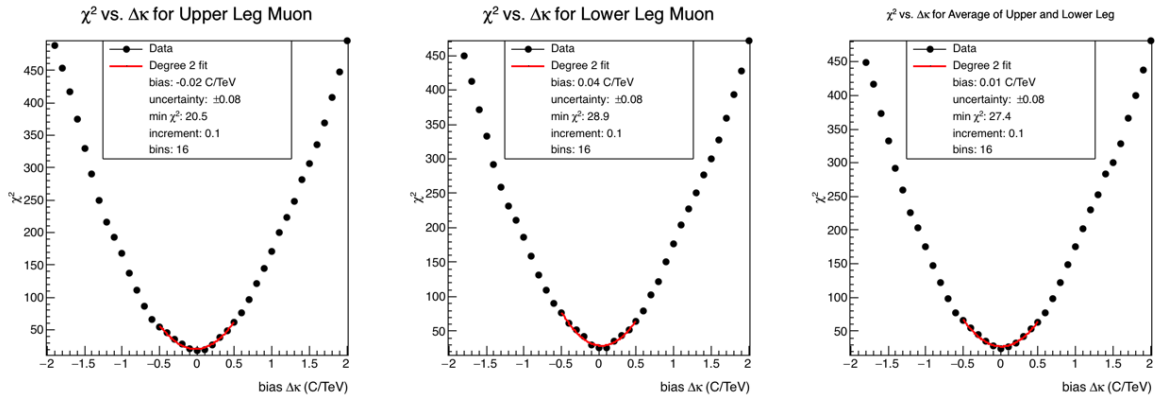

Figure 8: Testing Muon Track Dependence

Another consideration when running the Cosmic Endpoint Method is the cost to benefit ratio of normalizing the positive and negative muons separately. Although it would be statistically preferable to account for the imbalance in the number of positive and negative muons, this imbalance may not be significant enough to merit an increase in computational runtime of the code running the analysis. A comparison of the results when using one scaling factor versus two scaling factors is presented in Figure 9. For the case of normalizing all of the muons together, the bias was 0.03 ± 0.06 C/TeV, whereas in the case of normalizing the positive and negative muons separately, the bias was 0.04 ± 0.08 C/TeV. These values are remarkably close, indicating that it is not necessary to normalize the positive and negative muons separately.

Lastly, the impact of using a constant versus dynamic scale was evaluated. Each time a bias is injected into the simulation data, all of the curvature values are shifted, causing some that were within the cutoff range to exceed the upper limit, and some that were below the lower

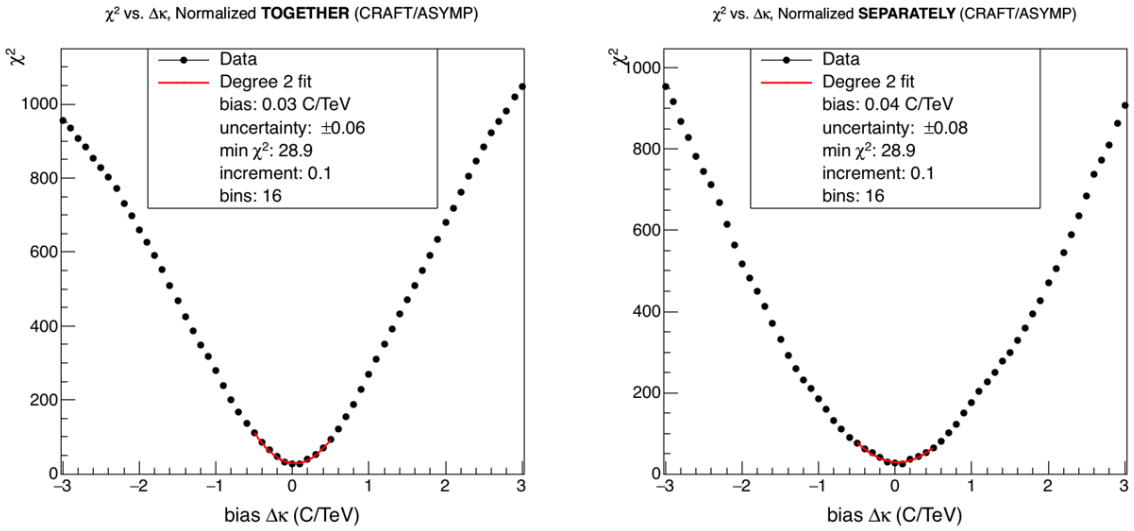

Figure 9: Comparison of Grouped vs. Differential Normalization of +/- Muons

cutoff to now be accepted into the region of interest. If the number of entries leaving the region of interest is not equal to the number of entries entering the region of interest, then a new scaling factor must be calculated after each applied shift to ensure that the number of entries in the simulation histogram is exactly equal to the number of entries in the smaller experimental data set. However, if one presumes that the number leaving and entering are approximately the same, then one can use the same scaling factor for all injected biases to save computational power. The results shown in the figure below indicate that this is indeed the case, and that one need not use a dynamically changing scale.

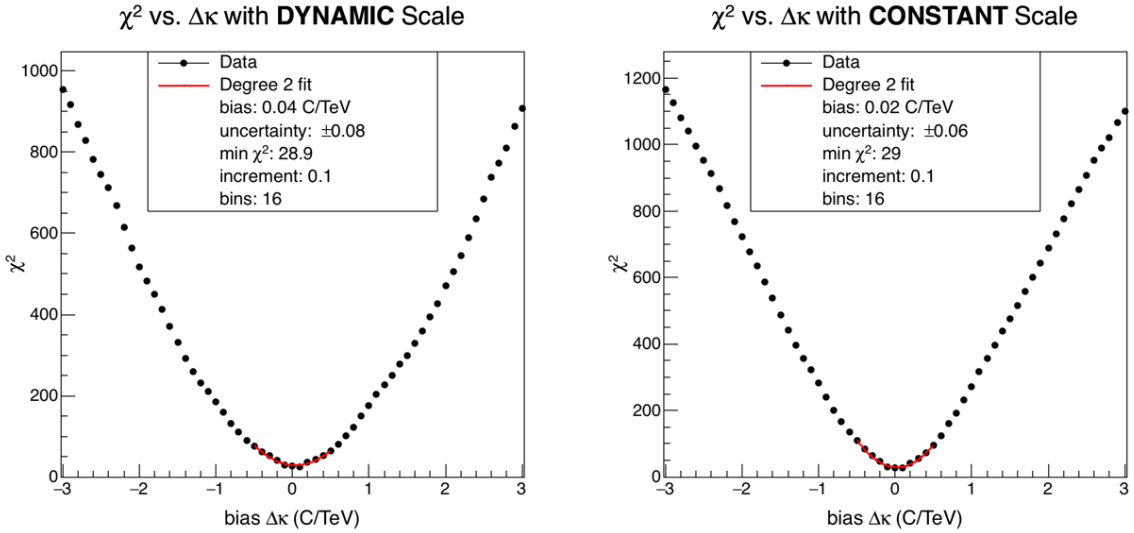

Figure 10: Comparison of Constant vs. Dynamic Scaling

3 Propagating p_T Uncertainty to Uncertainty in Dimuon Mass Yield

3.1 Background

Using the 2015 cosmic muon data, the Cosmic Endpoint Method demonstrated that there was some small apparent curvature bias in the detector. Because there is some uncertainty in this bias, this translates into some uncertainty in p_T, which can propagate into larger uncertainties in p_T-dependent variables. One such variable is the invariant mass. The concept of invariant mass comes from the energy-momentum relation,

$$E^2 = \left(m_0 c^2\right)^2 + (pc^2)^2 \tag{3}$$

where E represents the total energy of the system, p represents its total momentum, c represents the speed of light (which is equal to 1 in natural units), and m_0 is the rest mass, or invariant mass, of the system. Typically, the invariant mass is not a quantity that is measured, but one that is reconstructed from other measured variables. Thus, it is subject to the uncertainty of the variables used to calculate it.

The premise of the second study was to simulate $q\bar{q} \rightarrow \mu^+\mu^-$ events and analyze the effects of uncertainty in p_T on the reconstructed dimuon invariant mass spectrum. In the highly relativistic case ($E >> m$, $y \rightarrow \eta$), the dimuon invariant mass can be written in terms of p_T as follows[11]:

$$M = \sqrt{2p_{T_1}p_{T_2}\left(\cosh\left(\eta_1 - \eta_2\right) - \cos\left(\phi_1 - \phi_2\right)\right)} \tag{4}$$

This equation shows that the dimuon mass explicitly depends on the muons' transverse momentum. Any uncertainty in the p_T will translate into some uncertainty in dimuon mass, and thus cause uncertainty in the yield of the mass spectrum above a selected threshold mass. The reason the mass *spectrum* is considered rather than the raw invariant mass has to do with the nature of particle discovery. When two protons collide, a shower of secondary particles is created, which can give rise to a host of final states. Because new particles that have never been observed would comprise some small fraction of these final states, it makes sense to look for changes in the distribution of masses for all of the final states. In this particular case, the dimuon mass spectrum may contain evidence for compositeness, which is the theory that all leptons and hadrons are made up of smaller particles called preons. If such small particles existed, then some fraction of the $q\bar{q} \rightarrow \mu^+\mu^-$ process would undergo Contact Interaction in which no Z boson intermediate is required. This would cause the tail end of the spectrum to have a flatter distribution because of the production of higher-mass dimuons. However, if preons did not exist, then all of the $q\bar{q} \rightarrow \mu^+\mu^-$ events would occur via Z boson or virtual photon (γ^*) intermediate, which is a process called Drell-Yan. The dimuon spectrum for all Drell-Yan events has a steeper, which indicates that a higher majority of events produce low-mass dimuons[12]. A comparison of the two processes is shown in Figure 11.

3.2 Procedure

The premise of the study is to conduct a counting experiment to quantify the effect of uncertainty in p_T on the yield in the dimuon mass spectrum. First, $q\bar{q} \rightarrow \mu^+\mu^-$ events were generated in Pythia8 at a center of mass energy of 13 TeV. This was done for both the Drell-Yan and the compositeness model at different energy scales Λ. An example of these invariant mass spectra are shown in Figure 12.

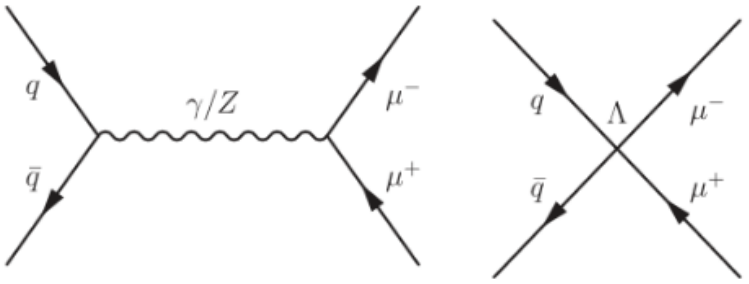

(a) Drell-Yan (b) Contact Interaction

Figure 11: **Drell-Yan vs. Contact Interaction**: In both processes, a quark and an antiquark produce two muons, but in the case of Contact Interaction, no boson intermediate is required. This theoretical interaction occurs at an energy scale Λ.

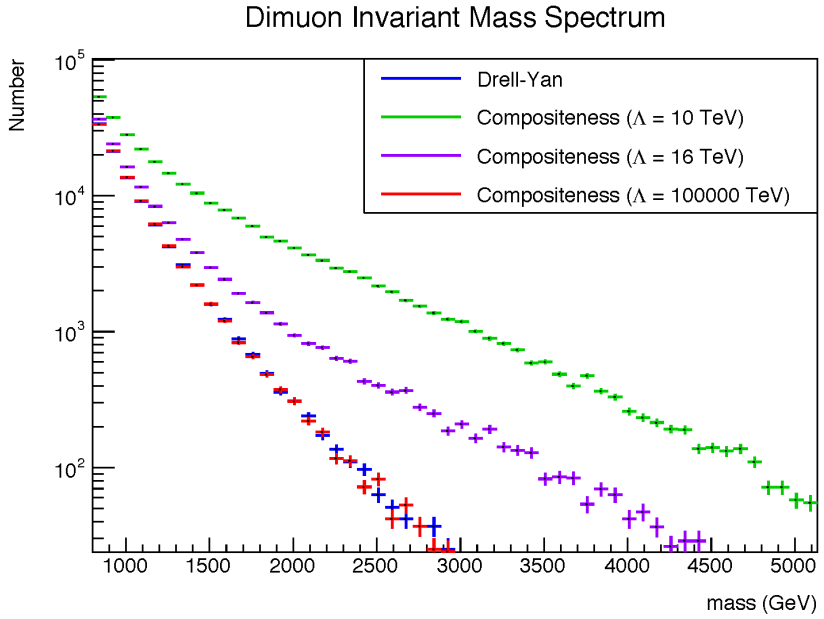

Figure 12: **Dimuon Invariant Mass Spectra**: The plot shows distributions for the dimuon invariant mass for the Drell-Yan case and the compositness model for different energy scales of compositeness. As the energy scale increases, the fewer Contact Interaction events occur, and the closer the distribution is to the Drell-Yan case.

The invariant mass plots were then reconstructed after taking into account the uncertainty in p_T. Because there are two factors of p_T in the dimuon mass formula in Eq. 4, one has the choice between scaling both factors p_T up, scaling both down, or scaling one up and one down. The amount of scaling may be determined for an arbitrary uncertainty in p_T, or one may use the results of the Cosmic Endpoint Method to convert the curvature bias into a p_T-dependent scaling factor. Thus, the two invariant mass spectra (one before scaling the p_T values and one after) may be compared for differences in yield. This comparison was done by selecting a minimum mass and counting the number of entries above and including that mass cut. This integral was performed for a series of mass cuts, and the relative difference between the counts

was plotted as a function of the minimum mass cut. The relative difference can be written as

$$\text{Relative Difference} = \frac{|\text{Shifted Integral} - \text{Unshifted Integral}|}{\text{Unshifted Integral}} \tag{5}$$

The plot of relative difference against the minimum mass gives a tentative estimate of uncertainty in yield caused by a curvature bias in the detector. This uncertainty will be different for different mass regions, and also differ depending on the type of scaling in p_T. Although the Cosmic Endpoint Method suggests that there is a monodirectional shift in curvature (which translates into a bi-directional shift in p_T), one can obtain the results of shifting both p_T values in the same direction to obtain a wider band of uncertainty in the yield.

3.3 Results

The results of this study indicate that the relative difference in the yield was quadratically dependent on the mass. This is to be expected since there are two factors of p_T that contribute to the invariant mass. The first is due to the p_T-dependent scaling factor in p_T, and the second is due to the fact that the dimuon mass is approximately proportional to p_T. An example of the relative difference as a function of the minimum mass for a 0.05 C/TeV curvature bias is shown in Figure 13.

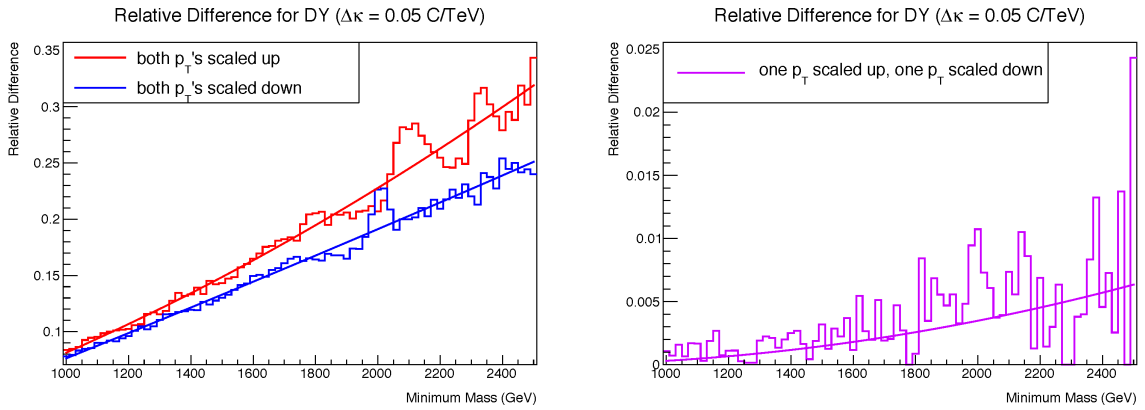

(a) Relative Difference for Bidirectional Shift in Curvature

(b) Relative Difference for Bidirectional Shift in Curvature

Figure 13: **Relative Difference vs. Minimum Mass**: These plots show that the relative difference between the invariant mass spectrum before scaling p_T and after scaling p_T increases with the minimum mass used to count entries. The different colored lines indicate the type of scaling applied to p_T.

As the plots in the figure above demonstrate, the relative difference in the counts increases with the minimum mass, which indicates that the uncertainty in yield is higher in the higher-mass regions of the spectrum. Furthermore, on the whole one obtains a greater relative difference when scaling both of the factors of p_T in the same direction as opposed to different directions. Thus, the maximum dimuon mass can be obtained by scaling both factors of p_T upwards, and the minimum dimuon mass can be obtained by scaling both factors of p_T downwards. This gives a sort of "yield uncertainty band" for the count of dimuons in a given mass region.

To obtain a more accurate representation of the yield uncertainty band, the actual results

of the Cosmic Endpoint Method may be used. The actual scaling factor may be obtained by converting both p_T values into curvature values, applying the shift in curvature, adding the uncertainty to the bias, and then reconverting the curvatures into a now scaled p_T. Because the bias was discovered to be 0.01 $\pm$0.07 C/TeV one should scale up by 0.08 C/TeV and scale down by 0.06 C/Tev. The scaled p_T values may then be used to remake the dimuon invariant mass spectrum and compare it to the original using the relative difference. The results for the pure Drell-Yan model and the compositeness model at 16 TeV are shown in Figure 14.

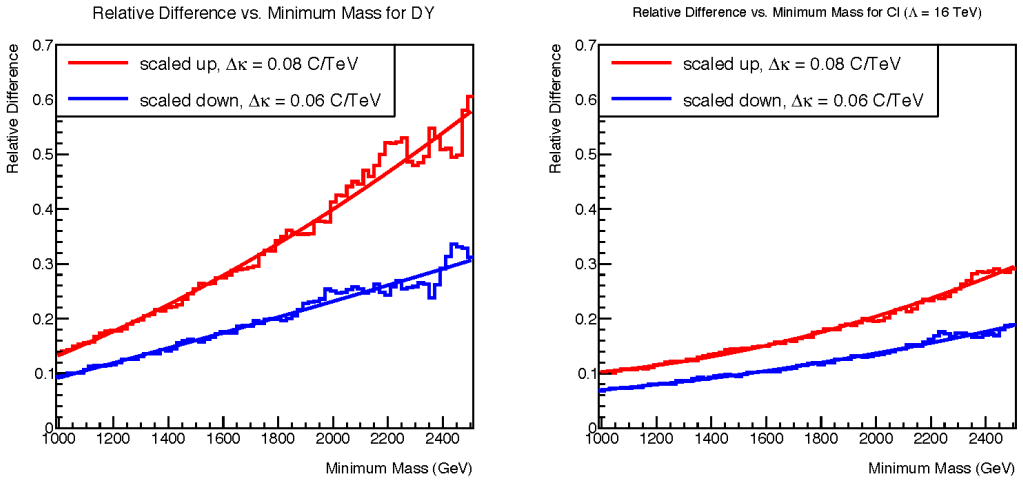

Figure 14: Maximum Yield Uncertainty Band for the DY and Compositeness Models

As the figure above shows, the relative difference is higher in the Drell-Yan case than in the compositeness model. This means that if actual collision data were subject to a constant bias in curvature, the difference between the actual invariant mass spectrum and the spectrum reconstructed from the p_T data is higher in the DY case. This means that uncertainty in yield differentially affects the non-compositeness and compositeness models, which should be taken into account in the search for compositeness.

4 Conclusions

These first study used a statistical tool called the Cosmic Endpoint Method to show evidence for some small curvature bias in the CMS detector. While this bias is almost inconsequential, the uncertainty in this bias translates into uncertainty in p_T, which can propagate into larger errors in the p_T-dependent properties of muons. One such property is the dimuon invariant mass, which is analyzed in $q\bar{q} \rightarrow \mu^+\mu^-$ events. By applying the curvature bias in the form of scaling p_T, one can quantify the uncertainty in yield in the mass spectrum. The results show that the relative difference in yield before and after taking the uncertainty in p_T into account increases quadratically with the minimum mass being considered. Thus, when searching for evidence of compositeness in the dimuon mass spectrum, the larger uncertainty present in the higher-mass regions cannot be ignored.

Citations

[1] https://home.cern/about/experiments/cms

[2] http://cms.web.cern.ch/news/how-cms-detects-particles

[3] http://cms.web.cern.ch/news/silicon-pixels

[4] http://cms.web.cern.ch/news/electromagnetic-calorimeter

[5] http://cms.web.cern.ch/news/hadron-calorimeter

[6] https://cdsweb.cern.ch/record/1279137/files/TRK-10-004-pas.pdf

[7] https://indico.cern.ch/event/173674/contributions/277733/attachments/219822/307886/mpogEndpointKypreos.pdf

[8] http://www.physics.rutgers.edu/ugrad/389/muon/muonphysics.pdf

[9] https://eddata.fnal.gov/lasso/summerstudents/papers/2015/Carmen-Giugliano.pdf

[10] https://arxiv.org/pdf/1206.4071.pdf

[11] https://indico.fnal.gov/getFile.py/access?contribId=2&resId=0&materialId=paper&confId=10225

[12] http://arxiv.org/pdf/1212.4563v2.pdf

Image References

[1] https://inspirehep.net/record/1409615/files/thesis.pdf

[2] http://www.particlecentral.com/accelerator_page.html

[3] https://inspirehep.net/record/867205/files/Figure_002.png

Acknowledgments

First, I would like to thank my supervisors Dr. Pushpalatha Bhat and Dr. Leonard Spiegel for their mentorship and unwavering support throughout this project. Next, I would like to thank Shawn Zaleski of Wayne State University for his willingness to entertain my endless stream of questions, for it is this kind of patience that fosters the best learning environment. I would like to express my utmost gratitude to the SIST program for giving me the opportunity to conduct research at Fermilab this summer. Lastly, I would like to thank my friends and family who have encouraged the curiosity that got me here in the first place.

A Curvature Bias as a $\mathbf{P_T}$ Dependent Shift in $\mathbf{P_T}$

Given that the curvature κ is equal to q/p_{T} where q is the charge and $\mathrm{p_T}$ is the transverse momentum, a biased or shifted value of curvature can be written as:

$$\begin{aligned}
\kappa' &= \kappa + \Delta\kappa \\
\frac{q}{{p_{\mathrm{T}}}'} &= \frac{q}{p_{\mathrm{T}}} + \Delta\kappa \\
\frac{1}{{p_{\mathrm{T}}}'} &= \frac{1}{p_{\mathrm{T}}} + \frac{\Delta\kappa}{q} \\
{p_{\mathrm{T}}}' &= \left(\frac{1}{p_{\mathrm{T}}} + \frac{\Delta\kappa}{q}\right)^{-1} \\
{p_{\mathrm{T}}}' &= \left(1 + \frac{\Delta\kappa\ p_{\mathrm{T}}}{q}\right)^{-1} \left(\frac{1}{p_{\mathrm{T}}}\right)^{-1}
\end{aligned}$$

For a small enough bias $\Delta\kappa$, the above expression can be simplified using a first-order binomial approximation as follows:

$$\begin{aligned}
{p_{\mathrm{T}}}' &\approx \left(1 - \frac{\Delta\kappa\ p_{\mathrm{T}}}{q}\right) \left(\frac{1}{p_{\mathrm{T}}}\right)^{-1} \\
{p_{\mathrm{T}}}' &\approx p_{\mathrm{T}} \left(1 - \frac{\Delta\kappa\ p_{\mathrm{T}}}{q}\right)
\end{aligned}$$

Because the charge q of a muon is always ± 1, the above expression can be rewritten as

$${p_{\mathrm{T}}}' \approx p_{\mathrm{T}} \left(1 \pm \Delta\kappa\ p_{\mathrm{T}}\right)$$

which is of the form

$${p_{\mathrm{T}}}' = \alpha p_{\mathrm{T}}$$

where α is the scaling factor. Since the shift $\Delta\kappa$ is a constant, the scaling factor α is linearly dependent on $\mathrm{p_T}$.

B Motivation for the Definition of Curvature

The *magntidue* of the magnetic force on any moving charged particle can be expressed as

$$F_B = q v_\perp B$$

where $v_\perp$ represents the velocity component of the particle tangential to the magnetic field. Because the force acts perpendicular to both the particle's trajectory and the magnetic field, the charged particle will travel in a curved path. Thus, one may set this force equal to the centripetal force for uniform circular motion, as shown below:

$$q v_\perp B = \frac{m v_\perp^2}{r}$$

Solving for r yields,

$$\begin{aligned}
r &= \frac{m v_\perp}{qB} \\
r &= \frac{p_{\mathrm{T}}}{qB}
\end{aligned}$$

In this case, the quantity $mv_{\perp}$ represents the momentum of the particle perpendicular to the magnetic field, which in the case of a muon traveling in the detector, is the transverse momentum of the muon. As the equation shows, the radius of curvature is proportional to the transverse momentum and inversely proportional to the charge of the muon. The smaller the radius of curvature, the more the particle is deflected, and the larger the radius, the less the particle is deflected. Taking into account only the variables that are dependent on the muon's properties, one can define a quantity called curvature κ which is simply the inverse of the radius:

$$\kappa = \frac{q}{p_{\mathrm{T}}}$$